

Supporting Information

Differential Stabilities and Sequence-Dependent Base Pair Opening Dynamics of Watson-Crick Base Pairs with 5-Hydroxymethylcytosine, 5-Formylcytosine, or 5-Carboxylcytosine

Marta W. Szulik^{1*}, Pradeep S. Pallan², Boguslaw Nocek³, Markus Voehler¹, Surajit Banerjee⁴, Sonja C. Brooks⁵, Andrzej Joachimiak³, Martin Egli², Brandt F. Eichman⁵, and Michael P. Stone^{1*}

¹Department of Chemistry, Vanderbilt Institute of Chemical Biology, Vanderbilt Ingram Cancer Center, and Center for Structural Biology, Vanderbilt University, Nashville, TN 37235

²Department of Biochemistry, Vanderbilt Institute of Chemical Biology, and Center for Structural Biology, School of Medicine, Vanderbilt University, Nashville, TN 37232

³Bioscience Division, Argonne National Laboratory, Argonne, IL 60439

⁴Northeastern Collaborative Access Team and Department of Chemistry and Chemical Biology, Cornell University, Argonne National Laboratory, Argonne, IL 60439

⁵Department of Biological Sciences, Vanderbilt Institute of Chemical Biology, and Center for Structural Biology, Vanderbilt University, Nashville, TN 37235

To whom correspondence should be addressed:

michael.p.stone@vanderbilt.edu

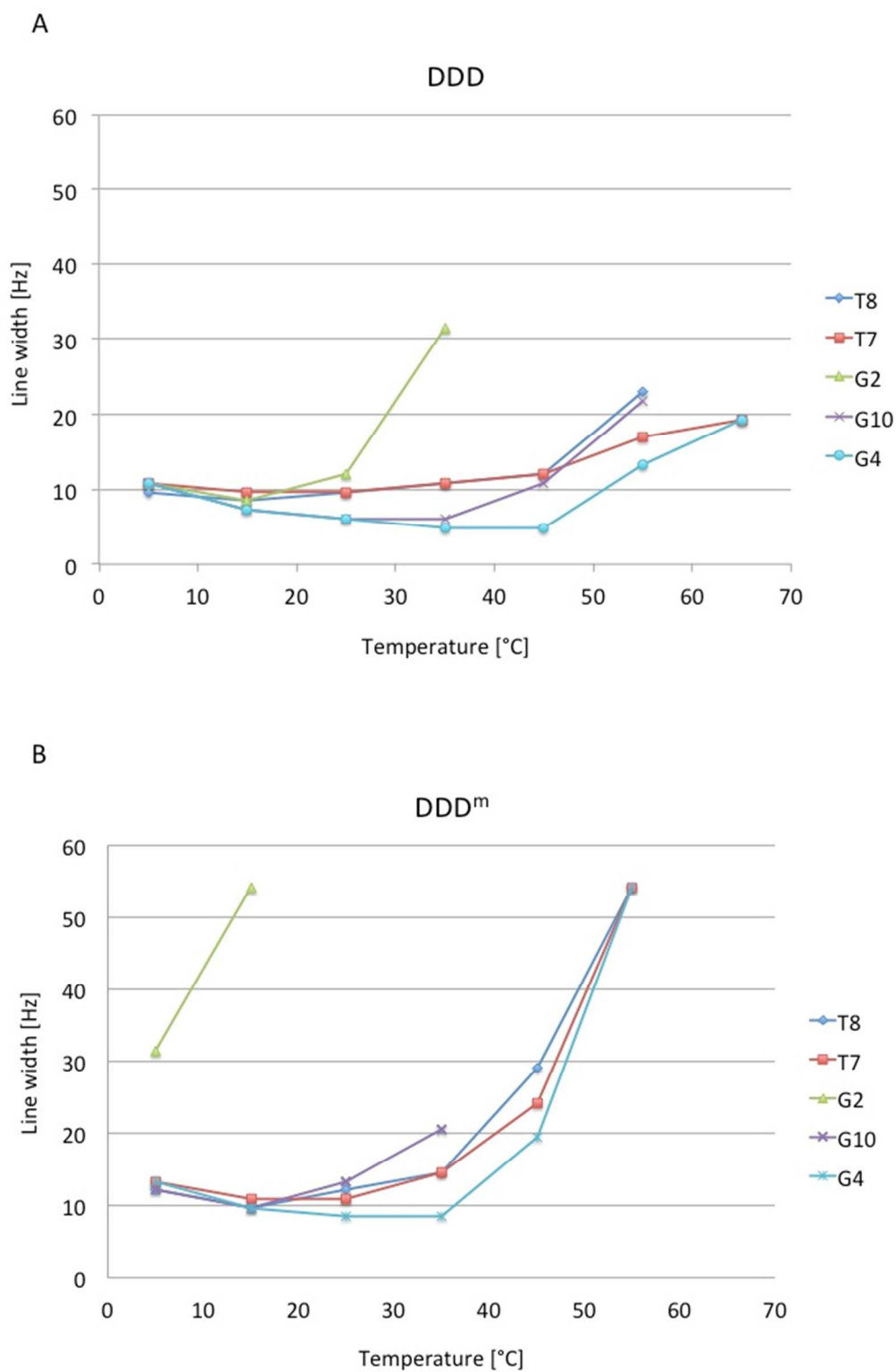
Table of Contents

Table S1.	Crystallization conditions for the DDD ^{hm} , DDD ^f and DDD ^{ca} duplexes.	3
Figure S1.	Temperature dependence of line widths of the imino proton resonances of the DDD, DDD ^m , DDD ^{hm} , DDD ^f and DDD ^{ca} duplexes.	4
Figure S2.	Modification site of the DDD ^{hm} displaying dual conformers of the 5hmC modified base and its interactions with surrounding waters and residues.	7
Figure S3.	Modification site of the DDD ^{hm} displaying interactions between the modified 5hmC and 3'-flanking G ²² through water molecules.	8
Figure S4.	Expanded plots from the aromatic-anomeric region of the NOESY spectra, depicting sequential NOE connectivities of (A) DDD, (B) DDD ^m , (C) DDD ^{hm} , (D) DDD ^f and (E) DDD ^{ca} duplexes.	9

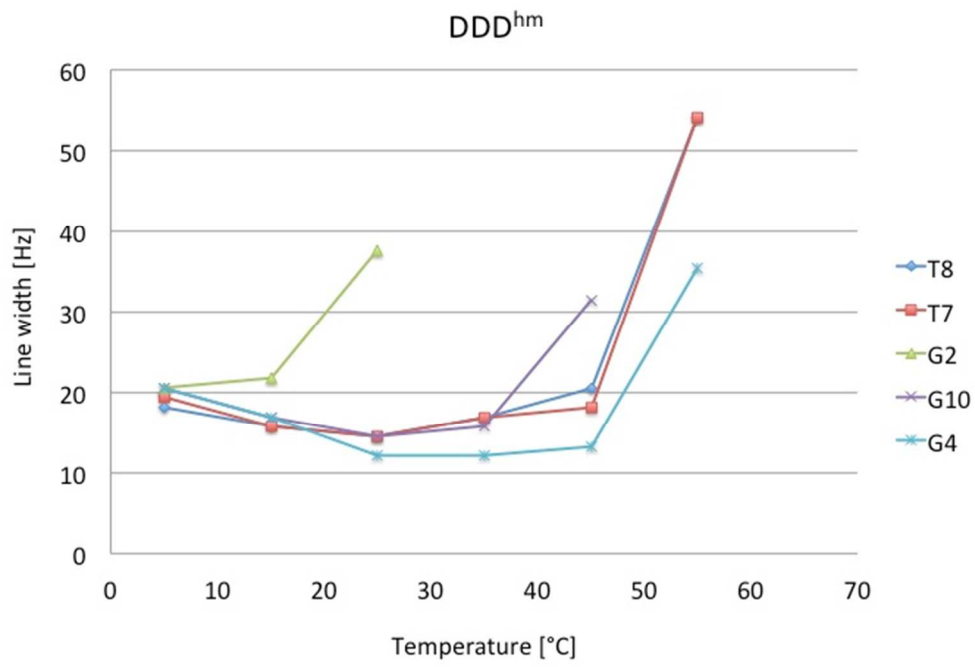
Table S1. Crystallization conditions.

Condition	DDD ^{hm}	DDD ^f	DDD ^{ca}
pH	7.0	6.0	6.0
Buffer	40 mM Na Cacodylate	40 mM Na Cacodylate	40 mM Na Cacodylate
Salts	80 mM NaCl, 20 mM MgCl ₂	80 mM NaCl	80 mM SrCl ₂
Additives	12 mM spermine 4HCl	12 mM spermine 4HCl	12 mM spermine 4HCl
2-methyl-2,4-pentanediol (MPD)	10 % (v/v)	10 % (v/v)	10 % (v/v)

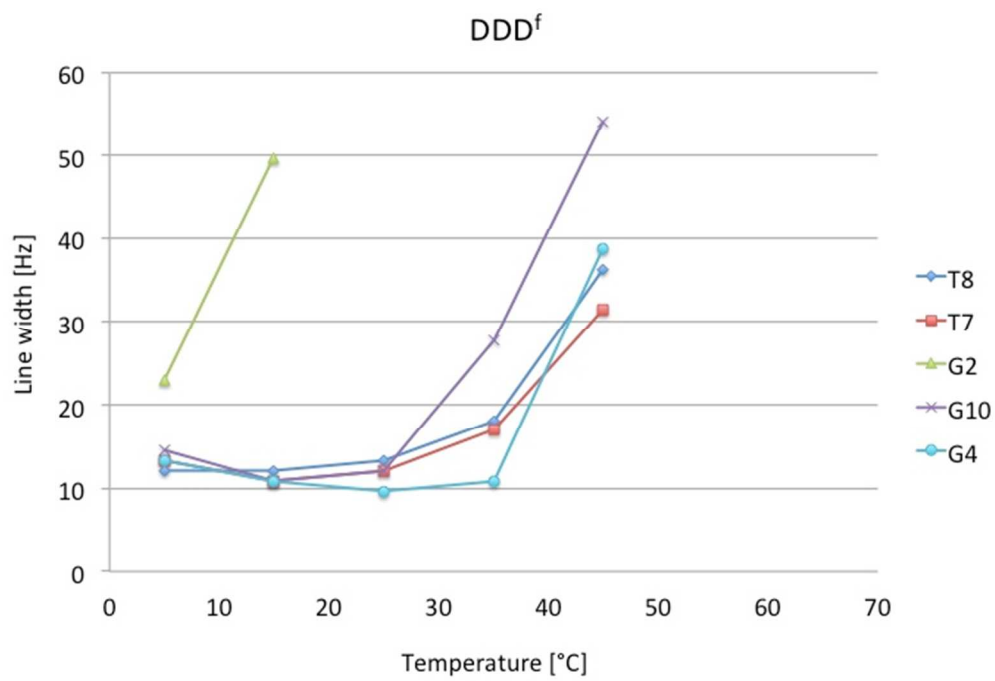
Figure S1. Temperature dependence of line widths of the imino proton resonances of the (A) DDD, (B) DDD^m, (C) DDD^{hm}, (D) DDD^f and (E) DDD^{ca} duplexes.



C



D



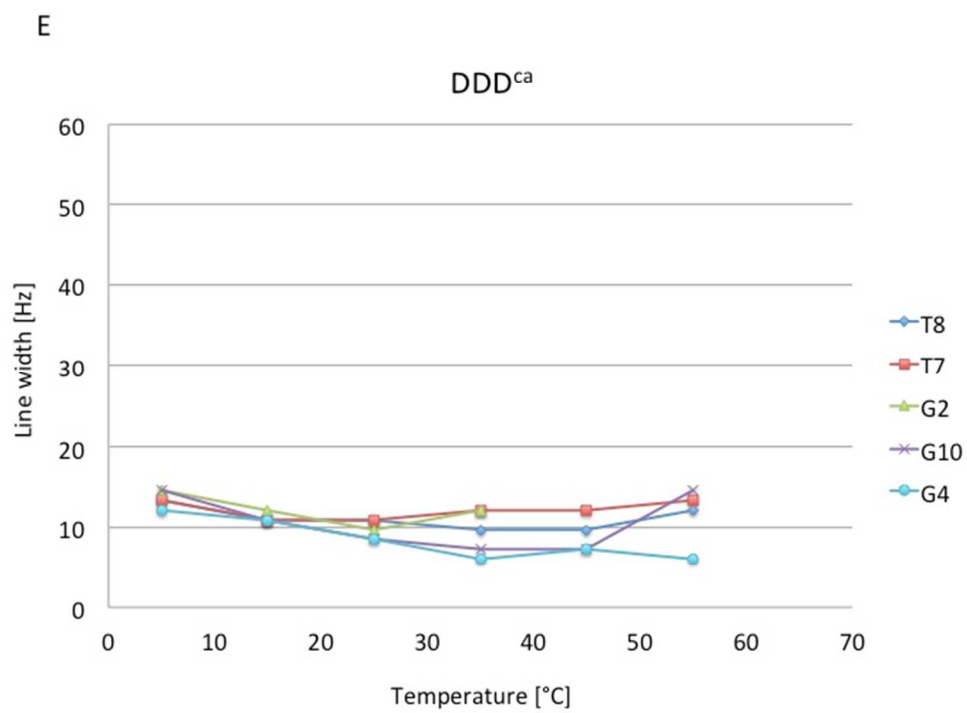


Figure S2. Modification site of the DDD^{hm} displaying dual conformers of the 5hmC modified base and its interactions with surrounding waters and residues.

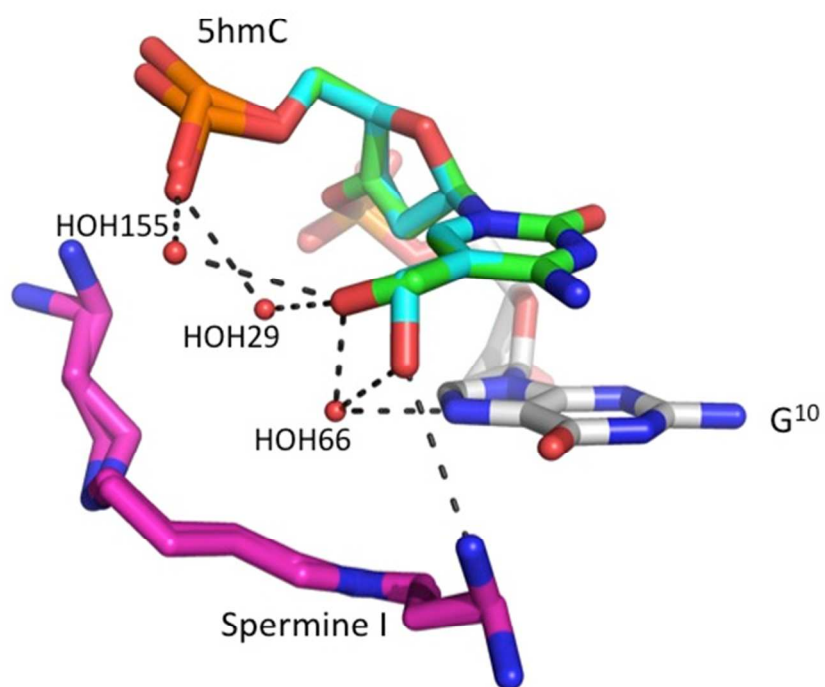


Figure S3. Modification site of the DDD^{hm} displaying interactions between the modified 5hmC and 3'-flanking G²² through water molecules.

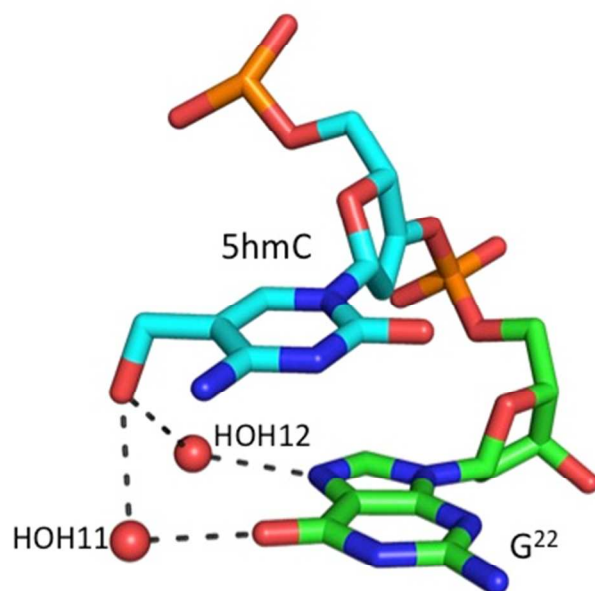


Figure S4. Expanded plots from the aromatic-anomeric region of the NOESY spectra, depicting sequential NOE connectivities of (A) DDD, (B) DDD^m, (C) DDD^{hm}, (D) DDD^f and (E) DDD^{ca} duplexes.

Data were collected at 900 MHz.

